



Chinese Pharmaceutical Association  
Institute of Materia Medica, Chinese Academy of Medical Sciences

Acta Pharmaceutica Sinica B

[www.elsevier.com/locate/apsb](http://www.elsevier.com/locate/apsb)  
[www.sciencedirect.com](http://www.sciencedirect.com)



ORIGINAL ARTICLE

# Exogenous phosphatidic acid reduces acetaminophen-induced liver injury in mice by activating hepatic interleukin-6 signaling through inter-organ crosstalk



Melissa M. Clemens<sup>a,b</sup>, Stefanie Kennon-McGill<sup>c</sup>, Joel H. Vazquez<sup>a,b</sup>, Owen W. Stephens<sup>d</sup>, Erich A. Peterson<sup>d</sup>, Donald J. Johann<sup>d</sup>, Felicia D. Allard<sup>e</sup>, Eric U. Yee<sup>e</sup>, Sandra S. McCullough<sup>f</sup>, Laura P. James<sup>f</sup>, Brian N. Finck<sup>g</sup>, Mitchell R. McGill<sup>a,c,h,\*</sup>

<sup>a</sup>Department of Pharmacology and Toxicology, College of Medicine, University of Arkansas for Medical Sciences, Little Rock, AR 72205, USA

<sup>b</sup>Interdisciplinary Graduate Program in Biomedical Sciences, Graduate School, University of Arkansas for Medical Sciences, Little Rock, AR 72205, USA

<sup>c</sup>Department of Environmental and Occupational Health, Fay W. Boozman College of Public Health, University of Arkansas for Medical Sciences, Little Rock, AR 72205, USA

<sup>d</sup>Winthrop P. Rockefeller Cancer Institute, University of Arkansas for Medical Sciences, Little Rock, AR 72205, USA

<sup>e</sup>Department of Pathology, Renaissance School of Medicine, Stony Brook University, Stony Brook, NY 11794, USA

<sup>f</sup>Department of Pediatrics, College of Medicine, University of Arkansas for Medical Sciences, Little Rock, AR 72205, USA

<sup>g</sup>Division of Geriatrics and Nutritional Sciences, Department of Internal Medicine, Washington University School of Medicine, St. Louis, MO 63110, USA

<sup>h</sup>Center for Dietary Supplement Research, University of Arkansas for Medical Sciences, Little Rock, AR 72205, USA

Received 11 March 2021; received in revised form 26 July 2021; accepted 17 August 2021

\*Corresponding author. Tel.: +1 501 526 6696.

E-mail address: [mmcgill@uams.edu](mailto:mmcgill@uams.edu) (Mitchell R. McGill).

Peer review under responsibility of Chinese Pharmaceutical Association and Institute of Materia Medica, Chinese Academy of Medical Sciences.

<https://doi.org/10.1016/j.apsb.2021.08.024>

2211-3835 © 2021 Chinese Pharmaceutical Association and Institute of Materia Medica, Chinese Academy of Medical Sciences. Production and hosting by Elsevier B.V. This is an open access article under the CC BY-NC-ND license (<http://creativecommons.org/licenses/by-nc-nd/4.0/>).

**KEY WORDS**

Acute liver injury;  
Acute liver failure;  
Adipokine;  
Cytokine;  
Dietary supplement;  
Drug-induced liver injury;  
Hepatotoxicity;  
Lipid

**Abstract** We previously demonstrated that endogenous phosphatidic acid (PA) promotes liver regeneration after acetaminophen (APAP) hepatotoxicity. Here, we hypothesized that exogenous PA is also beneficial. To test that, we treated mice with a toxic APAP dose at 0 h, followed by PA or vehicle (Veh) post-treatment. We then collected blood and liver at 6, 24, and 52 h. Post-treatment with PA 2 h after APAP protected against liver injury at 6 h, and the combination of PA and *N*-acetyl-L-cysteine (NAC) reduced injury more than NAC alone. Interestingly, PA did not affect canonical mechanisms of APAP toxicity. Instead, transcriptomics revealed that PA activated interleukin-6 (IL-6) signaling in the liver. Consistent with that, serum IL-6 and hepatic signal transducer and activator of transcription 3 (Stat3) phosphorylation increased in PA-treated mice. Furthermore, PA failed to protect against APAP in IL-6-deficient animals. Interestingly, IL-6 expression increased 18-fold in adipose tissue after PA, indicating that adipose is a source of PA-induced circulating IL-6. Surprisingly, however, exogenous PA did not alter regeneration, despite the importance of endogenous PA in liver repair, possibly due to its short half-life. These data demonstrate that exogenous PA is also beneficial in APAP toxicity and reinforce the protective effects of IL-6 in this model.

© 2021 Chinese Pharmaceutical Association and Institute of Materia Medica, Chinese Academy of Medical Sciences. Production and hosting by Elsevier B.V. This is an open access article under the CC BY-NC-ND license (<http://creativecommons.org/licenses/by-nc-nd/4.0/>).

**1. Introduction**

Acetaminophen (APAP) is a popular analgesic and antipyretic drug<sup>1</sup>, but overdose causes severe acute liver injury. In fact, it is currently the leading cause of acute liver failure (ALF) throughout much of the world<sup>2</sup>. Conversion of APAP to the reactive metabolite *N*-acetyl-*p*-benzo quinoneimine (NAPQI) initiates the hepatotoxicity. NAPQI binds to free sulfhydryl groups on cysteine residues, depleting hepatic glutathione and damaging proteins<sup>3–5</sup>. The protein binding leads to mitochondrial dysfunction and oxidative stress<sup>6,7</sup>, which activates the c-Jun N-terminal kinases 1/2 (JNK) and other kinases<sup>8–10</sup>. Activated JNK then translocates from the cytosol to mitochondria, where it exacerbates the mitochondrial dysfunction by reducing mitochondrial respiration<sup>9,11</sup>. Eventually, the mitochondrial permeability transition occurs<sup>12,13</sup> and the mitochondrial damage causes release of endonucleases from mitochondria, which then cleave nuclear DNA<sup>14</sup>. The affected hepatocytes die by necrosis<sup>15–17</sup>.

Phosphatidic acid (PA) is a critically important lipid in all prokaryotic and eukaryotic cells. It is the simplest diacylated glycerophospholipid, having a bare phosphate head group. In cell and organelle membranes, the small size and negative charge of the head group likely promotes negative curvature that may be important for membrane fission<sup>18</sup>. It is also a major metabolic intermediate, serving as a key precursor for synthesis of all other phospholipids, as well as triglycerides<sup>19</sup>. Finally, it is a major lipid second messenger with roles in nutrient sensing and cell proliferation *via* mechanistic target of rapamycin (mTOR) signaling<sup>19–21</sup>.

We recently demonstrated that PA is beneficial after APAP-induced liver injury in mice through an entirely novel mechanism<sup>22,23</sup>. Briefly, we found that endogenous PA is elevated in the liver and plasma after APAP overdose in both mice and humans, and that it promotes cell proliferation and therefore liver regeneration by regulating glycogen synthase kinase 3 $\beta$  (GSK3 $\beta$ )<sup>22,23</sup>. However, we did not test the effect of administering exogenous PA on APAP-induced liver injury. In the present study, we hypothesized that exogenous PA is similarly beneficial in a mouse model of APAP overdose.

**2. Materials and methods****2.1. Animals**

Age- and cage-matched male wild-type (WT) C57Bl/6J mice and *Il-6* knockout mice (*Il-6* KO; B6.129S2-*Il6*<sup>tm1Kopf/J</sup>) on the C56Bl/6J background between the ages of 8 and 12 weeks were obtained from The Jackson Laboratory (Bar Harbor, ME, USA). Female mice were not used because they are less susceptible to APAP hepatotoxicity<sup>24</sup>, which does not reflect the human phenotype<sup>25</sup>. The mice were housed in a temperature-controlled 12 h light/dark cycle room and allowed free access to food and water. The APAP and PA solutions were prepared fresh on the morning of each experiment. APAP was prepared by dissolving 15 mg/mL APAP (Sigma, St. Louis, MO, USA) in 1  $\times$  phosphate-buffered saline (PBS) with gentle heating and intermittent vortexing. The PA solution was prepared by re-constituting purified egg PA extract (Avanti Polar Lipids, Alabaster, AL, USA) at 10 mg/mL in 10% DMSO in 1  $\times$  PBS and warming to 80  $^{\circ}$ C for 20–30 min with intermittent vortexing to obtain a uniform hazy suspension, and cooling to approximately body temperature immediately before injection. To determine if PA affects liver injury, WT mice ( $n = 5–10$  per group) were fasted overnight then injected (i.p.) with 250 mg/kg APAP at 0 h, followed by 10% dimethylsulfoxide (DMSO) vehicle (Veh) or 20 mg/kg PA (i.p.) at 2 h. Blood and liver tissue were collected at 4 h (for JNK activation) or 6 h (other endpoints). We chose the 20 mg/kg dose of PA because it is commonly recommended when taken as a dietary supplement in humans. To determine if the combination of *N*-acetyl-L-cysteine (NAC) and PA reduces injury compared to NAC alone, some mice were injected with APAP at 0 h followed by 300 mg/kg NAC (dissolved in 1  $\times$  PBS) and either PA or Veh at 2 h ( $n = 7$  per group). Blood was collected at 6 h. We chose the 300 mg/kg dose of NAC because it is approximately 2-fold greater than the typical loading dose in humans after APAP overdose. Using this high dose of NAC ensures that our results comparing NAC with APAP + NAC are conservative and robust. For transcriptomics, the original PA experiment was repeated at the 6 h time point with addition of a Veh-only control group ( $n = 5$  per group). To determine if PA protection depends upon IL-6, the

experiment was repeated again at the 6 h time point using *Il-6* KO mice ( $n = 5-6$  per group) and WT mice matched for source, genetic background, age, diet, and environment, with a similar but higher dose of APAP (350 mg/kg). The change in APAP dose in the latter experiment was due to an adjustment made to our university animal use protocol during the course of the study and unrelated to our data from these experiments. Finally, to test the role of Kupffer cells, the original PA experiment was repeated at the 6 h time point with WT mice ( $n = 10$  per group) after 24 h i.v. (tail vein) pre-treatment with 0.2 mL of 17 mmol/L liposomal clodronate (Clodrosome, Brentwood, TN, USA). All study protocols were approved by the Institutional Animal Care and Use Committee of the University of Arkansas for Medical Sciences (Little Rock, AR, USA).

## 2.2. Subcellular fractionation

Right and caudate liver lobes were homogenized in ice cold isolation buffer containing 220 mmol/L mannitol, 70 mmol/L sucrose, 2.5 mmol/L HEPES, 10 mmol/L EDTA, 1 mmol/L ethylene glycol tetra-acetic acid, and 0.1% bovine serum albumin (pH 7.4) using a Thermo Fisher Bead Mill (Thermo Fisher, Waltham, MA, USA). Subcellular fractions were obtained by differential centrifugation. Samples were centrifuged at  $2500 \times g$  for 10 min to blood cells and debris. Supernatants were then centrifuged at  $20,000 \times g$  for 10 min to pellet mitochondria. The supernatant was retained as the cytosol fraction. Pellets containing mitochondria were then re-suspended in 100  $\mu$ L of isolation buffer and freeze-thawed three times using liquid nitrogen to disrupt the mitochondrial membranes. Protein concentration was measured in both the mitochondrial and cytosol fractions using the bicinchoninic acid (BCA) assay, and the samples were used for Western blot as described below.

## 2.3. Clinical chemistry

Alanine aminotransferase (ALT) was measured in serum using a kit from Point Scientific Inc. (Canton, MI, USA) according to the manufacturer's instructions.

## 2.4. Histology

Liver tissue sections were fixed in 10% formalin. For hematoxylin & eosin (H&E) staining, fixed tissues were embedded in paraffin wax, and then 5  $\mu$ m sections were mounted on glass slides and stained according to a standard protocol. Necrosis was quantified in the H&E-stained sections by two independent, fellowship-trained, hepatobiliary pathologists who were both blinded to sample identity. Percent necrosis was then averaged for each animal. For oil red O staining, fixed tissues were embedded in optimal cutting temperature (OCT) compound and rapidly frozen by placing on a metal dish floating in liquid nitrogen. 8  $\mu$ m sections were cut and mounted on positively-charged glass slides. The sections were allowed to dry for 30 min at room temperature, then treated with 60% isopropanol for 5 min, followed by freshly prepared oil red O solution in isopropanol for 10 min, and then 60% isopropanol for an additional 2 min. The sections were then rinsed with PBS, treated with Richard-Allan Gill 2 hematoxylin solution (Thermo Fisher) for 1 min, and rinsed again with PBS before cover-slipping. Digital images were taken using a Labomed Lx400 microscope with digital camera (Labo American Inc., Fremont, CA, USA).

## 2.5. Western blot

Liver tissues were homogenized in homogenizing buffer composed of 25 mmol/L HEPES buffer with 5 mmol/L EDTA, 0.1% CHAPS, and protease inhibitors (pH 7.4; Sigma). Protein concentration was measured using a BCA assay. The samples were then further diluted in homogenization buffer, mixed with reduced Laemmli buffer (Bioworld, Dublin, OH, USA), and boiled for 1 min. Equal amounts (60  $\mu$ g protein) were added to each lane of a 4%–20% Tris-glycine gel. After electrophoresis, proteins were transferred to polyvinylidene fluoride (PVDF) membranes and blocked with 5% milk in Tris-buffered saline with 0.1% Tween 20. Primary monoclonal antibodies were purchased from Cell Signaling Technology (Danvers, MA, USA): phospho-JNK (Cat. No. 4668), JNK (Cat. No. 9252), apoptosis-inducing factor (AIF; Cat. No. 5318), cytochrome *c* (Cat. No. 11940), GSK3 $\beta$  (Cat. No. 9315), phospho-GSK3 $\beta$  (Cat. No. 9323), and  $\beta$ -actin (Cat. No. 4967). All primary antibodies were used at 1:1000 dilution. Secondary antibodies were purchased from LiCor Biosciences (Lincoln, NE, USA): IRDye 680 goat anti-mouse IgG (Cat. No. 926-68070) and IRDye 800CW goat anti-rabbit IgG (Cat. No. 926-32211). All secondary antibodies were used at 1:10,000 dilution. Bands were visualized using the Odyssey Imaging System (LiCor Biosciences, Lincoln, NE, USA).

## 2.6. Glutathione measurement

Total glutathione (GSH + GSSG) and oxidized glutathione (GSSG) were measured using a modified Tietze assay, as we previously described in detail<sup>26</sup>.

## 2.7. APAP–protein adduct measurement

APAP–protein adducts were measured using high pressure liquid chromatography (HPLC) with electrochemical detection, as previously described<sup>27,28</sup>.

## 2.8. Transcriptomics

The Supporting Information contains all details concerning RNA sequencing sample prep, next generation sequencing, and bioinformatics analyses.

## 2.9. Statistics

Normality was assessed using the Shapiro–Wilk test. Normally distributed data were analyzed using Student's *t*-test for comparison of two groups or one-way ANOVA with *post-hoc* Student–Neuman–Keul's for comparison of three or more groups. Data that were not normally distributed were analyzed using a nonparametric Mann–Whitney U test for comparison of two groups, or one-way ANOVA on ranks with *post-hoc* Dunnet's test to compare three or more. All statistical tests were performed using SigmaPlot 12.5 software (Systat, San Jose, CA, USA).

## 3. Results

### 3.1. Exogenous PA reduces liver injury at 6 h after APAP overdose

To determine the effect of exogenous PA treatment on APAP-induced liver injury, we treated mice with APAP at 0 h followed

by PA or Veh control at 2 h. We then collected blood and liver tissue at 6 h (Fig. 1A). We observed a significant reduction in serum ALT values in the PA-treated mice at 6 h post-APAP (Fig. 1B). Two blinded, fellowship-trained hepatobiliary and GI pathologists independently evaluated histology slides and the results confirmed the reduction in injury (Fig. 1C and D).

NAC is the current standard-of-care treatment for APAP-induced liver injury in patients. To determine if the combination of NAC and PA can further reduce injury after APAP overdose compared to NAC alone, we treated mice with APAP followed by Veh, 300 mg/kg NAC and Veh, or 300 mg/kg NAC and 20 mg/kg PA. Post-treatment with NAC + Veh reduced serum ALT compared to APAP + Veh and the combination of NAC and PA reduced it further (Fig. 1E). The latter result confirms that PA protects against APAP and indicates that it has potential to be useful as an adjunct treatment with NAC for APAP overdose.

Finally, to determine if the protection at 6 h is persistent or represents a delay in injury, we treated mice with APAP at 0 h followed by either Veh or PA at 2 h and measured serum ALT at 24 h. We found that the protection with PA was lost at 24 h (Supporting Information Fig. S1). It is possible that additional early treatments or continuous PA infusion would still provide protection at 24 h and beyond, but these data indicate that the specific PA treatment regimen used here delays severe injury but does not prevent it. Altogether, these data demonstrate that exogenous PA could be an effective adjunct treatment with NAC to reduce early APAP hepatotoxicity or to extend the treatment window.

### 3.2. Exogenous PA does not affect the canonical mechanisms of APAP-induced liver injury

Next, we sought to determine the mechanisms by which exogenous PA reduces early APAP hepatotoxicity. The initiating step in APAP-induced liver injury is formation of the reactive metabolite *N*-acetyl-*p*-benzoquinone imine (NAPQI), which depletes

glutathione and binds to proteins, initiating the downstream oxidative stress that activates JNK. Importantly, we chose a 2 h post-treatment with PA to avoid any effect on APAP metabolism and bioactivation because it is known that NAPQI formation and protein binding is complete by approximately 1.5 h<sup>28</sup>. Nevertheless, to confirm that the decrease in liver injury at 6 h was not due to an effect on NAPQI formation, we measured total glutathione (GSH + GSSG) and APAP–protein adducts in the liver. We did not detect a significant difference between the APAP + Veh and APAP + PA groups in either parameter (Fig. 2A and B).

To determine if PA protects by preventing the early mitochondrial dysfunction and oxidative stress after APAP overdose, we measured GSSG in the liver. There was no significant difference in either total GSSG or the percentage of glutathione in the form of GSSG (%GSSG) between the two groups (Fig. 2C and D). JNK is activated by reactive oxygen species (ROS) after APAP overdose and worsens the mitotoxicity, so to further test the effect of PA on oxidative stress and to determine if JNK activation was altered, we immunoblotted for phosphorylated and total JNK. Again, we could not detect a difference between the APAP + Veh and APAP + PA groups at either 6 h or even 4 h, which is closer to the peak of JNK activation after APAP (Fig. 2E). To determine if PA had an effect on mitochondrial damage downstream of JNK, and therefore mitochondrial rupture, we also immunoblotted for AIF and cytochrome *c* release into cytosolic fractions, and again no differences were detected (Fig. 2F). Because we previously found that endogenous PA can regulate GSK3 $\beta$  activity through Ser9 phosphorylation<sup>23</sup> and because active GSK3 $\beta$  is known to exacerbate APAP-induced liver injury<sup>29</sup>, we also measured GSK3 $\beta$  Ser9 phosphorylation, but once again observed no differences (Fig. 2G). Finally, as an additional indicator of mitochondrial function, we measured triglycerides in the liver by both oil red O staining and direct biochemical measurement. Triglyceride accumulation after APAP overdose is a direct effect of mitochondrial dysfunction with resulting loss of mitochondrial fatty acid oxidation<sup>30</sup>, so a change in triglycerides can be

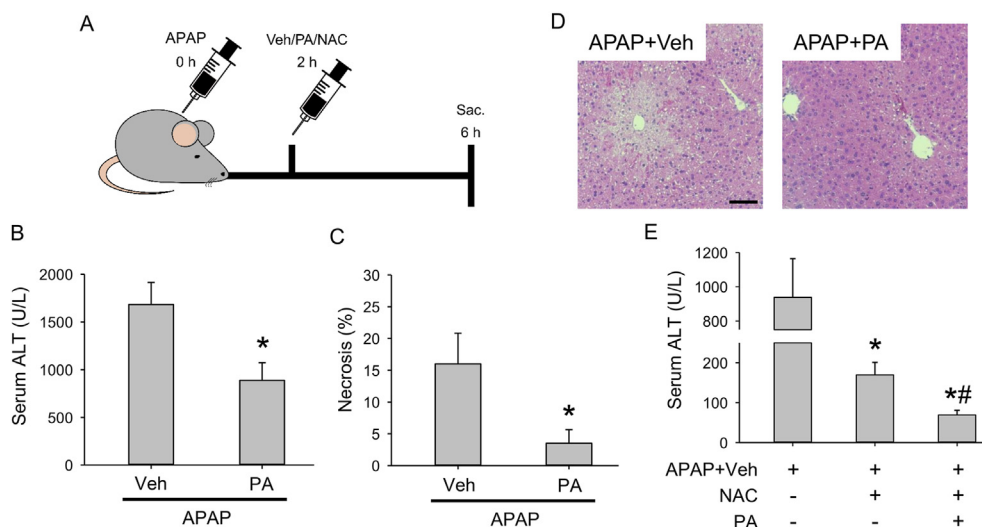


**Figure 1** Post-treatment with exogenous PA protects against early APAP hepatotoxicity. In one experiment, mice were treated with 250 mg/kg APAP at 0 h, followed by vehicle (Veh) or 20 mg/kg PA at 2 h. Blood and liver tissue were collected at 6 h. (A) Schematic of the treatment regimen. (B) Serum ALT activity. (C) Percent necrosis by area. (D) H&E-stained liver sections. In a second experiment, mice were treated with APAP + Veh at 0 h followed by NAC + Veh or NAC + PA at 2 h. Blood and liver tissue were collected at 6 h. Scale bar: 100  $\mu$ m. (E) Serum ALT. Data are expressed as mean  $\pm$  standard error (SE) for  $n = 5$ –10 per group. \* $P < 0.05$  vs. APAP + Veh. \*\* $P < 0.05$  vs. APAP + NAC.



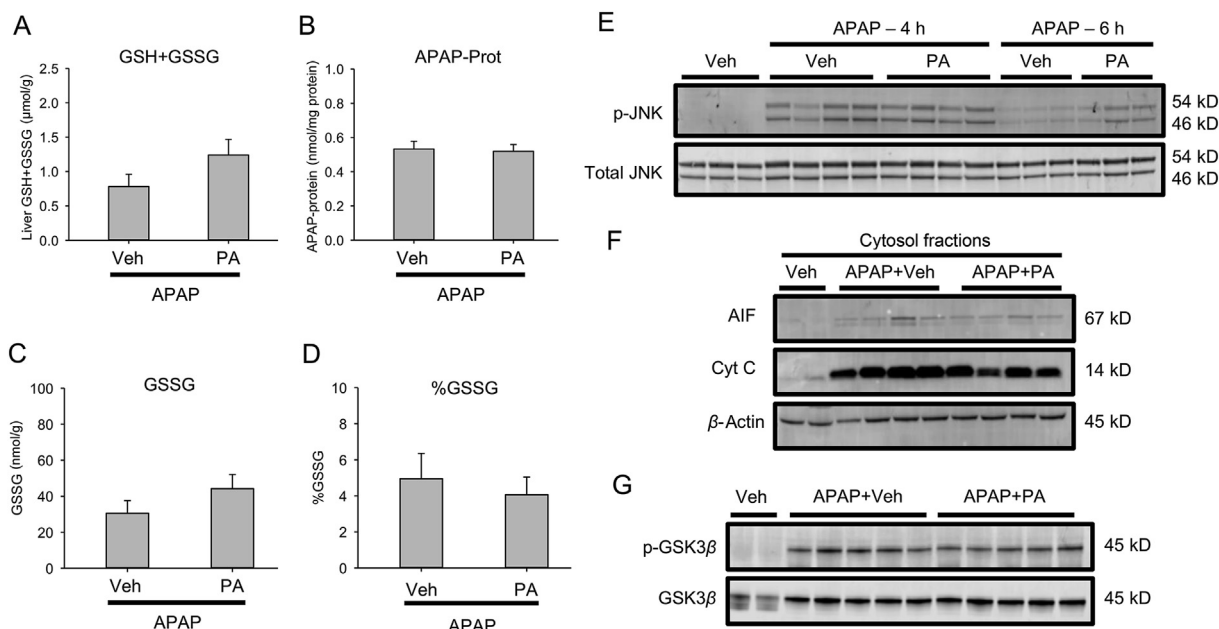


**Figure 2** Exogenous PA does not affect canonical mechanisms of APAP hepatotoxicity. Mice were treated with 250 mg/kg APAP at 0 h, followed by Veh or 20 mg/kg PA at 2 h. Liver tissue was collected at 6 h. (A) Total glutathione (GSH + GSSG) in liver. (B) APAP–protein adducts in liver. (C) Absolute oxidized glutathione (GSSG) in liver. (D) GSSG as the percentage of total glutathione (%GSSG) in the liver. (E) Immunoblots for total and phosphorylated JNK. (F) Immunoblots for AIF, cytochrome c, and  $\beta$ -actin. (G) Immunoblots for total and phosphorylated (Ser9) GSK3 $\beta$ . Data are expressed as mean  $\pm$  SE for  $n = 5$  per group. No statistically significant differences were detected.

considered a secondary endpoint for mitochondrial damage. Consistent with previous studies<sup>30–32</sup>, we observed oil red O accumulation in the damaged hepatocytes within centrilobular regions (Fig. 3A) and liver triglycerides were elevated in the APAP + Veh group compared to Veh treatment alone (Fig. 3B). However, again, we saw no difference between the APAP + Veh and APAP + PA groups. Altogether, these data largely rule out an effect of PA on APAP bioactivation, oxidative stress, and other effects downstream of oxidative stress, including JNK activation and mitochondrial damage.

### 3.3. Exogenous PA protects through IL-6 signaling in the liver

To identify other mechanisms by which PA might reduce early APAP hepatotoxicity, we performed next generation RNA sequencing in liver tissue from mice treated with Veh, APAP + Veh, and APAP + PA. We found that 6192 genes were differentially expressed between the Veh and APAP + Veh groups. Consistent with the protein alkylation, oxidative stress, and inflammation known to occur in APAP hepatotoxicity, gene ontology (biological processes; GO:BP) analysis revealed that genes involved in protein refolding, cell responses to chemical stimulus, and Toll-like receptor signaling were increased by APAP, while various cell growth and cell signaling processes were decreased (Fig. 4A). Only 388 genes were differentially expressed between the APAP + Veh and APAP + PA groups. This was insufficient for complete GO analysis, but it is notable that the GO:BP term “acute inflammatory response” was over-represented in the APAP + PA group when using a log 2 fold-change threshold of 1. Furthermore, hierarchical clustering analysis (Fig. 4B) and other measures (Supporting Information Figs. S2–S4) showed clear separation of the APAP + Veh and APAP + PA groups across the five biological replicates per group. Importantly,

Upstream Analysis using Ingenuity Pathway Analysis (IPA) software revealed activation of signaling downstream of IL-6 and its target transcription factor signal transducer and activator of transcription 3 (Stat3) (Table 1). Recent studies have demonstrated that IL-6 is protective in APAP hepatotoxicity<sup>33</sup>, and it was previously demonstrated that treatment with exogenous PA at doses similar to those we used here rapidly increase serum IL-6 concentration<sup>34</sup>. Thus, to confirm that PA increased serum IL-6 in our experiment, we measured IL-6 protein in serum at 6 h post-APAP. Importantly, IL-6 was significantly elevated in the APAP + PA mice compared to the APAP + Veh animals (Fig. 4C). Finally, to confirm activation of Stat3, we immunoblotted for phospho-Tyr705 Stat3 (p-Stat3) and total Stat3 in liver tissue. Consistent with our other results, p-Stat3 was significantly increased by PA treatment (Fig. 5A and B). Together, these data indicate that PA may protect against APAP toxicity by activating IL-6 and Stat3 signaling.

To confirm that exogenous PA reduces early APAP-induced liver injury through IL-6, we compared the effect of exogenously administered PA on APAP hepatotoxicity in WT and *Il-6* KO mice at 6 h post-APAP. Importantly, PA did not reduce liver injury in the KO mice, despite protecting in the WT mice in the same experiment (Fig. 6A–C). Areas of necrosis in liver tissue were the same between the APAP + Veh and APAP + PA treated *Il-6* KO mice (Fig. 6B and C), and serum ALT actually increased with PA treatment (Fig. 6A). In addition, ALT values were higher after APAP + Veh treatment in the *Il-6* KO mice compared to the WT mice matched for genetic background, age, diet, and environment (Fig. 6A). The latter is consistent with the recently proposed protective role of IL-6 in early APAP toxicity<sup>33</sup>, although it should be noted that there was no difference in area of necrosis after APAP + Veh treatment in the two genotypes, and that the WT and KO mice were not littermate controls. Altogether, these data

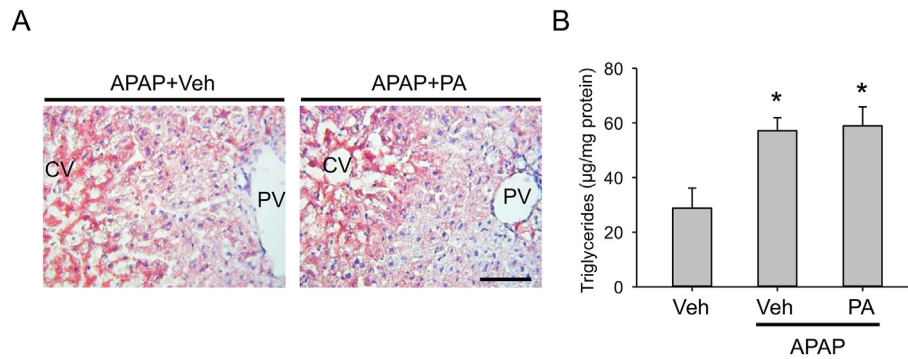


**Figure 3** Exogenous PA does not prevent loss of mitochondrial lipid oxidation. Mice were treated with 250 mg/kg APAP at 0 h, followed by Veh or 20 mg/kg PA at 2 h. Liver tissue was collected at 6 h. (A) Oil red O staining of liver sections. Scale bar: 100  $\mu\text{m}$ . (B) Liver triglycerides. PV, portal vein; CV, central vein. Data are expressed as mean  $\pm$  SE for  $n = 5$  per group. \* $P < 0.05$  vs. Veh.

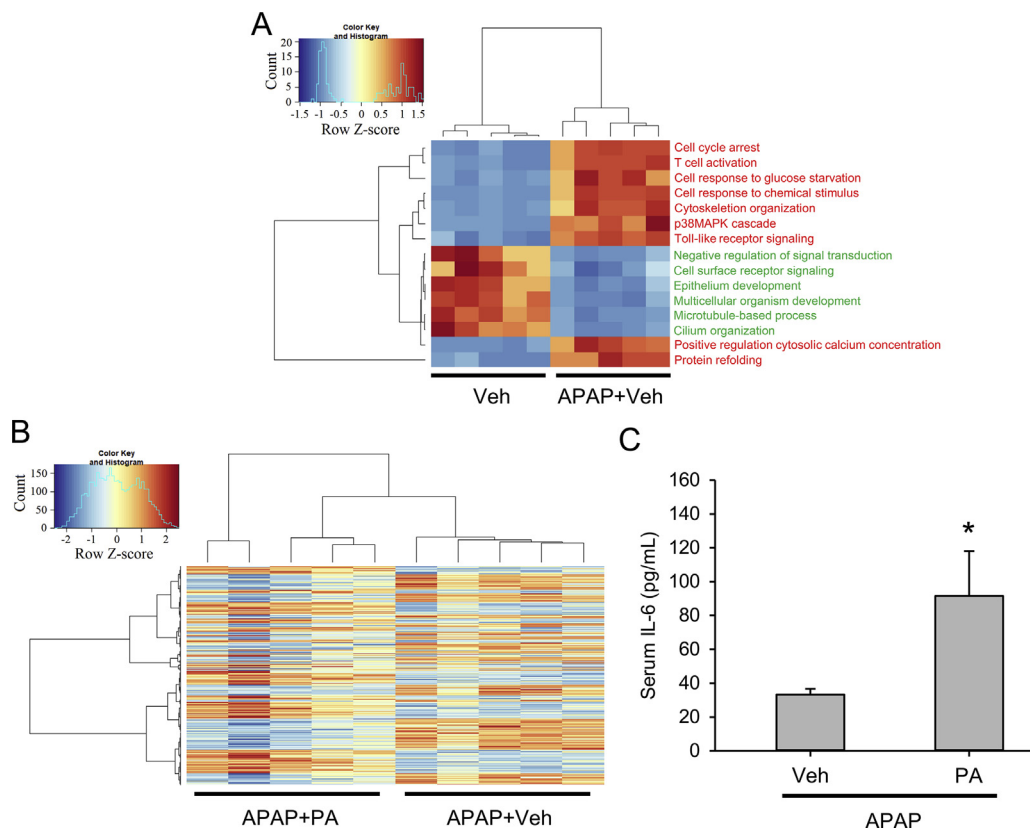


**Figure 4** Exogenous PA activates IL-6 signaling in the liver. Mice were treated with 250 mg/kg APAP or Veh alone at 0 h, followed by Veh or 20 mg/kg PA at 2 h. Blood and liver tissue were collected at 6 h. (A) Gene ontology (biological process) analysis of Veh alone vs. APAP + Veh. (B) Hierarchical clustering of genes in the APAP + Veh and APAP + PA groups. (C) Serum IL-6 values. Data are expressed as mean  $\pm$  SE for  $n = 5$  per group. \* $P < 0.05$  vs. APAP + Veh.

clearly demonstrate that IL-6 is necessary for the protection provided by exogenous PA in WT mice, and support previous work indicating that IL-6 is protective in APAP-induced liver injury overall.

#### 3.4. Adipose tissue is a likely source of increased IL-6 after PA treatment

Multiple liver cell types express IL-6, but Kupffer cells (KCs) are the major producers. To determine if the increase in IL-6 caused

by treatment with exogenous PA is due to increased expression of IL-6 in KCs or other liver cells, we measured *Il-6* mRNA in liver tissue in Veh-only, PA-only, APAP + Veh, and APAP + PA groups. Consistent with earlier work, *Il-6* expression increased in the liver after APAP overdose. However, we could not detect a significant difference in *Il-6* expression between the APAP + Veh and APAP + PA groups (Fig. 7A). Because KCs account for only a small portion of cells in the liver, it is possible that total liver mRNA has poor sensitivity to detect changes specifically within KCs. Thus, to further test if KCs are the source of IL-6 after PA

**Table 1** Signaling pathways affected by exogenous PA after APAP overdose.

Pathway	Predicted effect	Z-score	P-value
IL-6	Activated	3.346	0.0219
Stat3	Activated	3.0213	0.0132

treatment, we pre-treated mice with liposomal clodronate to ablate hepatic macrophages. The following day, we administered APAP followed by either PA or Veh. Blood and liver tissue were collected at 6 h post-APAP. Surprisingly, serum ALT was still significantly reduced by PA (Fig. 7B), despite depletion of the liver macrophages (Fig. 7C). These data once again confirm protection with PA and indicate that the liver itself is probably not the major source of IL-6 after PA treatment.

To identify other possible sources of IL-6, we treated mice with PA or Veh and collected liver, kidney, lung, epididymal white adipose tissue (eWAT), and spleen 4 h later. The experiment was designed to replicate earlier work showing that exogenous PA treatment increases circulating IL-6<sup>34</sup> but without exploring the source. We chose these specific tissues because they have high basal IL-6 expression and produce IL-6 in other disease contexts. Interestingly, we observed an 18-fold increase in *Il-6* mRNA in eWAT (Fig. 7D). We could not detect differences in any of the other tissues. To confirm these results at the protein level, we immunoblotted for IL-6 in both eWAT and liver tissue lysates. Consistent with the mRNA data, there was an increase in IL-6

protein in eWAT but not liver (Fig. 7E–G). These data are consistent with the idea that adipose tissue is a source of the increased systemic IL-6 after PA treatment, indicating inter-organ crosstalk between liver and fat in the protective mechanism of exogenous PA. However, the specific cell type responsible for the increased IL-6 (e.g., resident macrophages vs. adipocytes) is not clear from these data. Further studies are underway to determine that.

### 3.5. Exogenous PA does not promote liver regeneration

Finally, because we previously demonstrated that endogenous PA promotes liver regeneration<sup>22,23</sup> and because IL-6 is a well-known driver of that process<sup>35</sup>, we wanted to determine if exogenous PA enhances regeneration and repair after APAP overdose. To test that, we treated mice with APAP at 0 h, followed by exogenous PA or Veh at 6, 24, and 48 h post-APAP (Fig. 8A). We selected these late post-treatment time points to avoid an effect on the early injury at 6 h, which could have decreased liver regeneration secondary to the reduced injury. We then collected blood and liver tissue at 24 and 52 h. Although serum ALT was significantly decreased at 52 h (Fig. 8B), which is consistent with the overall protective effects of exogenous PA, there was no apparent difference in area of necrosis (Fig. 8C) and no change in proliferating cell nuclear antigen (Pcna, Fig. 8D) between the treatment groups at either time point. To determine if PA simply failed to increase IL-6 levels at these later time points, we measured serum IL-6 and found that there were no

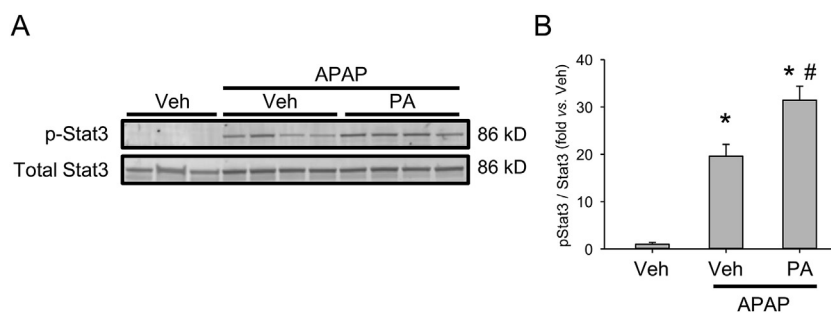


**Figure 5** Exogenous PA activates Stat3 in the liver. Mice were treated with 250 mg/kg APAP or Veh alone at 0 h, followed by Veh or 20 mg/kg PA at 2 h. Blood and liver tissue were collected at 6 h. (A) Immunoblots for phosphorylated (p-Tyr705) and total Stat3. (B) Densitometry. Data are expressed as mean  $\pm$  SE for  $n = 3$ –4 per group. \* $P < 0.05$  vs. Veh. # $P < 0.05$  vs. APAP + Veh.

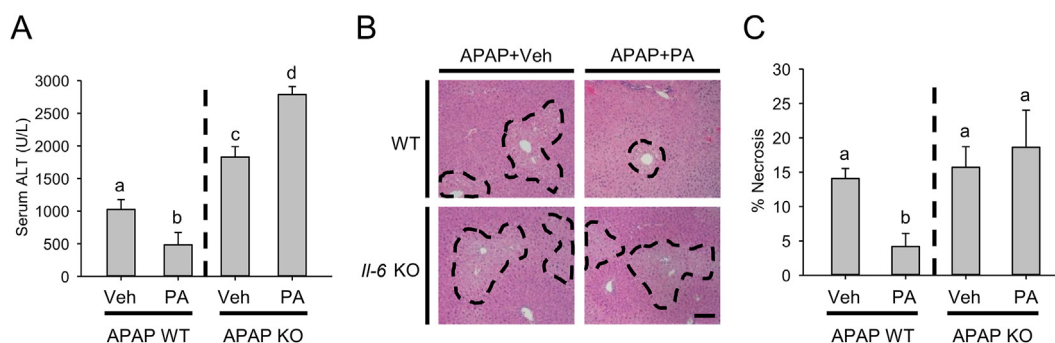


**Figure 6** Exogenous PA does not protect in *Il-6* KO mice. WT and *Il-6* KO mice were treated with 350 mg/kg APAP at 0 h, followed by Veh or 20 mg/kg PA at 2 h. Blood and liver tissue were collected at 6 h. (A) Serum ALT activity from both genotypes. (B) H&E-stained liver sections from both genotypes. Scale bar: 100  $\mu$ m. (C) Percent necrosis from the H&E-stained liver sections from both genotypes. Data are expressed as mean  $\pm$  SE for  $n = 5$ –6 per group. Groups with different letters (a, b, c, and d) are significantly different from each other ( $P < 0.05$ ).

statistically significant differences between the APAP + Veh and APAP + PA groups (Fig. 8E). There are a few possible interpretations of these data, but overall the results indicate that the exogenous PA treatment regimen that we used is ineffective for enhancing regeneration.

#### 4. Discussion

Together with our earlier work, the results from this study reveal that endogenous and exogenous PA have different beneficial effects in APAP hepatotoxicity, involving different mechanisms of action. We previously demonstrated that endogenous PA accumulates in liver tissue and plasma after APAP overdose in both mice and humans<sup>22</sup>. Importantly, inhibition of the PA accumulation had no effect on the early injury in mice but did reduce regeneration and survival by de-regulating GSK3 $\beta$  activity through an effect on Ser9 phosphorylation<sup>22,23</sup>. In the present study, we found that exogenous PA reduces or delays the early injury by increasing systemic IL-6 levels but has no effect on

GSK3 $\beta$  phosphorylation and minimal effect on liver regeneration. The latter may be because PA has a short half-life in serum, so more frequent treatments are needed to see an effect. It may also be because IL-6 expression and release is so high late after APAP overdose that further increases are not possible, though short half-life would also explain why the 2 h post-treatment delayed liver injury but did not provide protection at 24 h. Overall, these data indicate that exogenous PA or PA derivatives have potential to one day be a useful adjunct with NAC to treat early APAP hepatotoxicity in patients, but targeting PA-mediated signaling to promote liver regeneration in late presenters may require a different approach. The latter might also indicate that PA must be incorporated into membranes near Wnt receptors in order to alter GSK3 $\beta$  signaling and regeneration, rather than acting on lipid receptors in the cell membrane, such as lysoPA receptors (LPARs).

Our results are consistent with earlier data demonstrating that systemic administration of exogenous PA dramatically increases circulating levels of IL-6<sup>34</sup> and adds to those results by

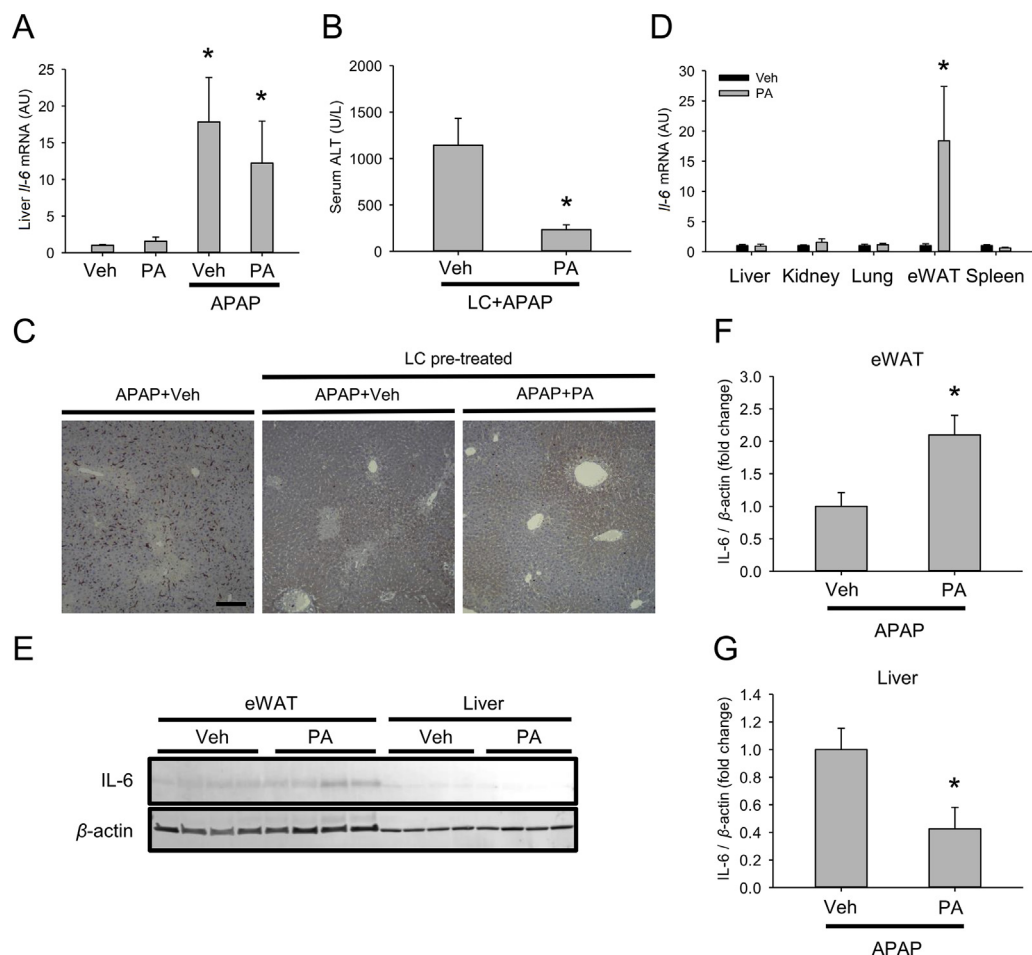


**Figure 7** The source of IL-6 after PA is extrahepatic and likely includes white adipose tissue. In one experiment, mice were treated with 250 mg/kg APAP at 0 h, followed by Veh or 20 mg/kg PA at 2 h. Where indicated, mice were pre-treated for 24 h with liposomal clodronate (LC). Blood and liver tissue were collected at 6 h. In a second experiment, mice were treated with 20 mg/kg PA or Veh and various tissues were collected 4 h later. (A) Liver *Il-6* mRNA from the first experiment. (B) Serum ALT activity from the experiment with LC pre-treatment. (C) F4/80 immunohistochemistry for macrophages in liver tissue sections from the experiment with LC pretreatment (dark brown puncta show positive staining). Scale bar: 100  $\mu$ m. (D) *Il-6* mRNA from the second experiment. (E) Immunoblot for IL-6 in eWAT and liver tissue from the second experiment. (F) Densitometry for IL-6 in eWAT. (G) Densitometry for IL-6 in liver tissue. Data are expressed as mean  $\pm$  SE for  $n = 5-10$  per group. \* $P < 0.05$  vs. APAP + Veh or vs. PBS.



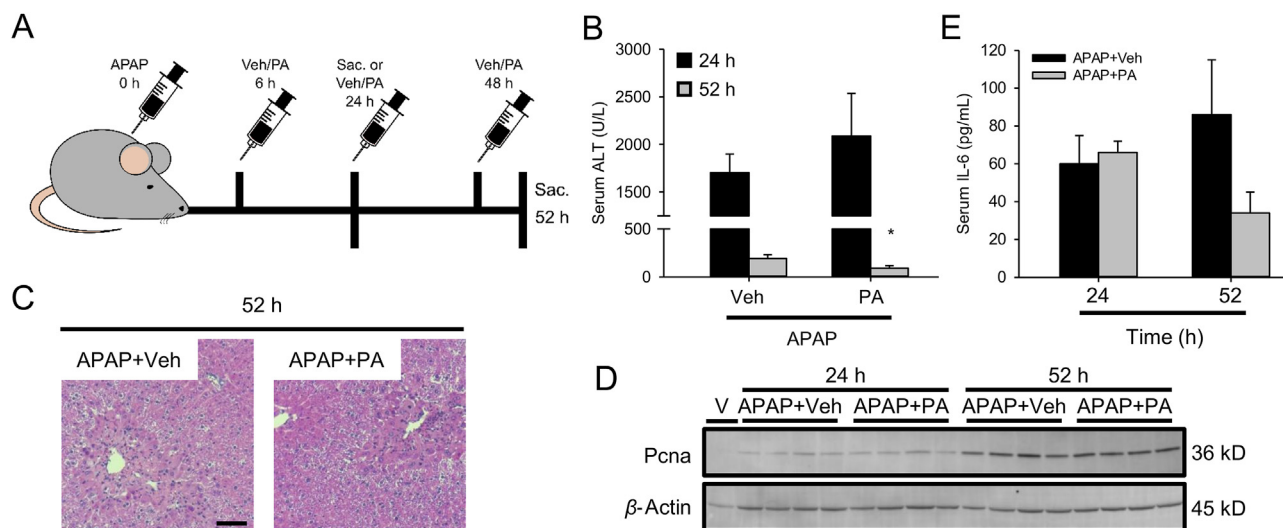


**Figure 8** Multiple post-treatment with exogenous PA does not affect liver regeneration. Mice were treated with 250 mg/kg APAP at 0 h, followed by Veh or 20 mg/kg PA at 6, 24, and 48 h. Blood and liver tissue were collected at 24 and 52 h. (A) Schematic depicting the treatment regimen. (B) Serum ALT. (C) H&E-stained liver sections. Scale bar: 100  $\mu$ m. (D) Immunoblot for proliferating cell nuclear antigen (Pcna) and  $\beta$ -actin. (E) Serum IL-6. Data are expressed as mean  $\pm$  SE for  $n = 4$ –5 per group. \* $P < 0.05$  vs. APAP + Veh.

demonstrating that adipose tissue is a likely source. Although we could not determine which specific cell type is responsible for the increased IL-6 production in eWAT from our data, it is likely to be adipose tissue-resident macrophages. Earlier studies revealed that directly treating the macrophage cell line RAW264.7 with PA *in vitro* increased expression of IL-6 and other cytokines in those cells with a time course that closely resembles *in vivo* induction<sup>34</sup>.

Our data also confirm the protective role of IL-6 in APAP hepatotoxicity. Masubuchi et al.<sup>36</sup> reported that *Il-6* KO mice have worse injury after APAP overdose. More recently, Gao et al.<sup>33</sup> observed that administration of exogenous IL-6 is protective. Although the mechanism by which IL-6 reduces APAP hepatotoxicity remains elusive, there are a few possibilities. IL-6 induces expression of heat shock protein 70 (Hsp70) and other Hsps in liver tissue after APAP overdose<sup>36</sup> and *Hsp70* KO worsens APAP toxicity<sup>37</sup>, so it is possible that PA ultimately protected through Hsps. In fact, Ni et al.<sup>38</sup> recently demonstrated that adducted proteins form toxic insoluble aggregates, and that inhibition of autophagy worsens APAP toxicity by reducing removal of those aggregates. Hsp70 has a central role in chaperone-mediated autophagy (CMA)<sup>39</sup>, so together these data may indicate that CMA is another critical autophagic process for removal of the adducted protein aggregates. However, we were unable to consistently detect an increase in either Hsp70 or Hsp40 in the APAP + PA group compared to the APAP + Veh group by immunoblotting (data not shown), so that seems unlikely. Another possibility is that IL-6 trans-signaling blocked the detrimental effects of IL-11. In a preprint, Dong et al.<sup>40</sup> recently reported that IL-11 may mediate APAP toxicity, that transgenic expression of HyperIL-6 (recombinant IL-6 with soluble IL-6 receptor) reduces APAP-induced liver injury, and that the protective effect of HyperIL-6 is lost in *Il-11* KO mice. However, considerably more research is needed to support that hypothesis.

Interestingly, Bae et al.<sup>41</sup> recently demonstrated that exogenously administered lysoPA also protects against APAP hepatotoxicity. PA can be converted to lysoPA by phospholipases, so it is

theoretically possible that lysoPA contributed to the protection we observed in our study. However, their data demonstrated that lysoPA protected by 1) preventing early glutathione depletion and increasing glutathione re-synthesis at 6 h post-APAP and by 2) altering JNK and GSK3 $\beta$  activation<sup>41</sup>. We could not detect any effect of exogenous PA on either glutathione or kinases in our experiments, so it is likely that PA protected through entirely different mechanisms in our study. Bae et al.<sup>41</sup> also used a 1-h pretreatment in most of their experiments, which has limited clinical relevance and makes it difficult to directly compare our results.

Initially, it was surprising to us that exogenous PA did not enhance liver regeneration after APAP overdose in our experiment despite multiple treatments. Our prior work demonstrated that endogenous PA is critical for normal liver regeneration<sup>22,23</sup>. Additionally, IL-6 is known to be very important in liver repair. *Il-6*-deficient animals have delayed regeneration after partial hepatectomy, APAP overdose, and CCl<sub>4</sub> hepatotoxicity<sup>42–45</sup>. On the other hand, Bajt et al.<sup>46</sup> found that injection of recombinant IL-6 does not enhance regeneration after APAP overdose, and many treatments that do enhance regeneration do not increase IL-6. It may be the case then that basal IL-6 levels are sufficient to aid liver repair, such that reducing IL-6 can blunt regeneration but increasing it has no effect. In our case, however, exogenous PA failed to affect serum IL-6 at later time points—likely due to the short half-life of PA—so we cannot determine if an increase in IL-6 would have been beneficial later. More data are needed to understand the details of those effects.

## 5. Conclusions

Overall, we conclude that post-treatment with exogenous PA reduces APAP hepatotoxicity in mice by increasing systemic IL-6, which is protective. Because PA is readily available over-the-counter as a supplement due to its purported ergogenic effects<sup>47</sup> and because the combination of PA and NAC protected better than NAC alone in our experiments, exogenous PA or PA derivatives may one day be a useful adjunct with NAC for treatment

of APAP overdose patients. However, more research is needed to test that possibility. In future studies, we will explore the effects of different doses, different acyl chain composition, and different PA formulations to optimize the protection. We will also test the effects of both endogenous and exogenous PA in other liver disease models.

### Acknowledgments

This study was funded in part by a 2018 Pinnacle Research Award from the AASLD Foundation, USA (Mitchell R. McGill); the Arkansas Biosciences Institute (Mitchell R. Mc Gill), which is the major research component of the Arkansas Tobacco Settlement Proceeds Act of 2000, USA; and the National Institutes of Health grants (USA) T32 GM106999 (Mitchell R. McGill and Joel H. Vazquez), R01 DK104735 (Brian N. Finck), R01 DK117657 (Brian N. Finck), R42 DK121652 (Brian N. Finck), R56 DK111735 (Brian N. Finck), R42 DK079387 (Laura P. James), UL1 TR003107 (Laura P. James and Stefanie Kennon-McGill), and TR003108 (Laura P. James and Stefanie Kennon-McGill). We are grateful for expert technical assistance provided by the Dept. of Laboratory Animal Medicine at UAMS, USA (especially Robin Mulkey) and by the Experimental Pathology Core, USA [especially Jennifer D. James, HT (ASCP), HTL, QIHC].

### Author contributions

Melissa M. Clemens, Brian N. Finck, and Mitchell R. McGill designed the study. Melissa M. Clemens, Stefanie Kennon-McGill, Joel H. Vazquez, Mitchell R. McGill, and Sandra S. McCullough performed experiments. Melissa M. Clemens, Mitchell R. McGill, Brian N. Finck, and Laura P. James analyzed and interpreted biochemical data. Owen W. Stephens, Erich A. Peterson, and Donald J. Johann collected and analyzed transcriptomics data. Felicia D. Allard and Eric U. Yee performed histopathological analyses. Melissa M. Clemens and Mitchell R. McGill drafted the manuscript. All authors revised the manuscript.

### Conflicts of interest

The authors declare no competing interests.

### Appendix A. Supporting information

Supporting data to this article can be found online at <https://doi.org/10.1016/j.apsb.2021.08.024>.

### References

- Kaufman DW, Kelly JP, Rosenberg L, Anderson TE, Mitchell AA. Recent patterns of medication use in the ambulatory adult population of the United States: the Slone survey. *J Am Med Assoc* 2002;**287**:337–44.
- Lee WM. Etiologies of acute liver failure. *Semin Liver Dis* 2008;**28**:142–52.
- Jollow DJ, Mitchell JR, Potter WZ, Davis DC, Gillette JR, Brodie BB. Acetaminophen induced hepatic necrosis. II. Role of covalent binding *in vivo*. *J Pharmacol Exp Therapeut* 1973;**187**:195–202.
- Mitchell JR, Jollow DJ, Potter WZ, Gillette JR, Brodie BB. Acetaminophen induced hepatic necrosis. IV. Protective role of glutathione. *J Pharmacol Exp Therapeut* 1973;**187**:211–7.
- McGill MR, Hinson JA. The development and hepatotoxicity of acetaminophen: reviewing over a century of progress. *Drug Metab Rev* 2020;**52**:472–500.
- Jaeschke H. Glutathione disulfide formation and oxidant stress during acetaminophen-induced hepatotoxicity in mice *in vivo*: the protective effect of allopurinol. *J Pharmacol Exp Therapeut* 1990;**255**:935–41.
- Cover C, Mansouri A, Knight TR, Bajt ML, Lemasters JJ, Pessayre D, et al. Peroxynitrite-induced mitochondrial and endonuclease-mediated nuclear DNA damage in acetaminophen hepatotoxicity. *J Pharmacol Exp Therapeut* 2005;**315**:879–87.
- Gunawan BK, Liu ZX, Han D, Hanawa N, Gaarde WA, Kaplowitz N. c-Jun N-terminal kinase plays a major role in murine acetaminophen hepatotoxicity. *Gastroenterology* 2006;**131**:165–78.
- Hanawa N, Shinohara M, Saberi B, Gaarde WA, Han D, Kaplowitz N. Role of JNK translocation to mitochondria leading to inhibition of mitochondria bioenergetics in acetaminophen-induced liver injury. *J Biol Chem* 2008;**283**:13565–77.
- Ramachandran A, McGill MR, Xie Y, Ni HM, Ding WX, Jaeschke H. Receptor interacting protein kinase 3 is a critical early mediator of acetaminophen-induced hepatocyte necrosis in mice. *Hepatology* 2013;**58**:2099–108.
- Win S, Than TA, Min RWM, Aghajan M, Kaplowitz N. c-Jun N-terminal kinase mediates mouse liver injury through a novel Sab (SH3BP5)-dependent pathway leading to inactivation of intra-mitochondrial Src. *Hepatology* 2016;**63**:1987–2003.
- Kon K, Kim JS, Jaeschke H, Lemasters JJ. Mitochondrial permeability transition in acetaminophen-induced necrosis and apoptosis of cultured mouse hepatocytes. *Hepatology* 2004;**40**:1170–9.
- Reid AB, Kurten RC, McCullough SS, Brock RW, Hinson JA. Mechanisms of acetaminophen-induced hepatotoxicity: role of oxidative stress and mitochondrial permeability transition in freshly isolated mouse hepatocytes. *J Pharmacol Exp Therapeut* 2005;**312**:509–16.
- Bajt ML, Cover C, Lemasters JJ, Jaeschke H. Nuclear translocation of endonuclease G and apoptosis-inducing factor during acetaminophen-induced liver cell injury. *Toxicol Sci* 2006;**94**:217–25.
- Gujral JS, Knight TR, Farhood A, Bajt ML, Jaeschke H. Mode of cell death after acetaminophen overdose in mice: apoptosis or oncotic necrosis?. *Toxicol Sci* 2002;**67**:322–8.
- McGill MR, Yan HM, Ramachandran A, Murray GJ, Rollins DE, Jaeschke H. HepaRG cells: a human model to study mechanisms of acetaminophen hepatotoxicity. *Hepatology* 2011;**53**:974–82.
- McGill MR, Sharpe MR, Williams CD, Taha M, Curry SC, Jaeschke H. The mechanism underlying acetaminophen-induced hepatotoxicity in humans and mice involves mitochondrial damage and nuclear DNA fragmentation. *J Clin Invest* 2012;**122**:1574–83.
- Kooijman EE, Chupin V, de Kruijff B, Burger KNJ. Modulation of membrane curvature by phosphatidic acid and lysophosphatidic acid. *Traffic* 2003;**4**:162–74.
- Pokotylo I, Kravets V, Martinec J, Ruelland E. The phosphatidic acid paradox: too many actions for one molecule class? Lessons from plants. *Prog Lipid Res* 2018;**71**:43–53.
- Fang Y, Vilella-Bach M, Flanigan A, Chen J. Phosphatidic acid-mediated activation of mitogenic mTOR signaling. *Science* 2001;**294**:1942–5.
- Foster DA. Phosphatidic acid and lipid-sensing by mTOR. *Trends Endocrinol Metab* 2013;**24**:272–8.
- Lutkewitte AJ, Schweitzer GG, Kennon-McGill S, Clemens MM, James LP, Jaeschke H, et al. Lipin deactivation after acetaminophen overdose causes phosphatidic acid accumulation in liver and plasma in mice and humans and enhances liver regeneration. *Food Chem Toxicol* 2018;**115**:273–83.
- Clemens MM, Kennon-McGill S, Apte U, James LP, Finck BN, McGill MR. The inhibitor of glycerol 3-phosphate acyltransferase FSG67 blunts liver regeneration after acetaminophen overdose by altering GSK3 $\beta$  and Wnt/ $\beta$ -catenin signaling. *Food Chem Toxicol* 2019;**125**:279–88.

24. Du K, Williams CD, McGill MR, Jaeschke H. Lower susceptibility of female mice to acetaminophen hepatotoxicity: role of mitochondrial glutathione, oxidant stress and c-jun N-terminal kinase. *Toxicol Appl Pharmacol* 2014;**281**:58–66.
25. Rubin JB, Hameed B, Gottfried M, Lee WM, Sarkar M. Acetaminophen-induced acute liver failure is more common and more severe in women. *Clin Gastroenterol Hepatol* 2018;**16**:936–46.
26. McGill MR, Jaeschke H. A direct comparison of methods used to measure oxidized glutathione in biological samples: 2-vinylpyridine and *N*-ethylmaleimide. *Toxicol Mech Methods* 2015;**25**:589–95.
27. Muldrew KL, James LP, Coop L, McCullough SS, Hendrickson HP, Hinson JA, et al. Determination of acetaminophen–protein adducts in mouse liver and serum and human serum after hepatotoxic doses of acetaminophen using high-performance liquid chromatography with electrochemical detection. *Drug Metab Dispos* 2002;**30**:446–51.
28. McGill MR, Lebofsky M, Norris HRK, Slawson MH, Bajt ML, Xie Y, et al. Plasma and liver acetaminophen–protein adduct levels in mice after acetaminophen treatment: dose-response, mechanisms, and clinical implications. *Toxicol Appl Pharmacol* 2013;**269**:240–9.
29. Shinohara M, Ybanez MD, Win S, Than TA, Jain S, Gaarde WA, et al. Silencing glycogen synthase kinase-3 $\beta$  inhibits acetaminophen hepatotoxicity and attenuates JNK activation and loss of glutamate cysteine ligase and myeloid cell leukemia sequence. *J Biol Chem* 2010;**285**:8244–55.
30. Hu J, Ramshesh VK, McGill MR, Jaeschke H, Lemasters JJ. Low dose acetaminophen induces reversible mitochondrial dysfunction associated with transient c-Jun N-terminal kinase activation in mouse liver. *Toxicol Sci* 2016;**150**:204–15.
31. Bhattacharyya S, Yan K, Pence L, Simpson PM, Gill P, Letzig LG, et al. Targeted liquid chromatography-mass spectrometry analysis of serum acylcarnitines in acetaminophen toxicity in children. *Biomark Med* 2014;**8**:147–59.
32. Borude P, Bhushan B, Gunewardena S, Akakpo J, Jaeschke H, Apte U. Pleiotropic role of p53 in injury and liver regeneration after acetaminophen overdose. *Am J Pathol* 2018;**188**:1406–18.
33. Gao RY, Wang M, Liu Q, Feng D, Wen Y, Xia Y, et al. Hypoxia-inducible factor (HIF)-2 $\alpha$  reprograms liver macrophages to protect against acute liver injury via the production of interleukin-6. *Hepatology* 2020;**71**:2105–17.
34. Lim HK, Choi YA, Park W, Lee T, Ryu SH, Kim SY, et al. Phosphatidic acid regulates systemic inflammatory responses by modulating the Akt-mammalian target of rapamycin-p70 S6 kinase 1 pathway. *J Biol Chem* 2003;**278**:45117–27.
35. Clemens MM, McGill MR, Apte U. Mechanisms and biomarkers of liver regeneration after drug-induced liver injury. *Adv Pharmacol* 2019;**85**:241–62.
36. Masubuchi Y, Bourdi M, Reilly TP, Graf ML, George JW, Pohl LR. Role of interleukin-6 in hepatic heat shock protein expression and protection against acetaminophen-induced liver disease. *Biochem Biophys Res Commun* 2003;**304**:207–12.
37. Tolson JK, Dix DJ, Voellmy RW, Roberts SM. Increased hepatotoxicity of acetaminophen in *Hsp70i* knockout mice. *Toxicol Appl Pharmacol* 2006;**210**:157–62.
38. Ni HM, McGill MR, Chao X, Du K, Williams JA, Xie Y, et al. Removal of acetaminophen protein adducts by autophagy protects against acetaminophen-induced liver injury in mice. *J Hepatol* 2016;**65**:354–62.
39. Cuervo AM, Wong E. Chaperone-mediated autophagy: roles in disease and aging. *Cell Res* 2014;**24**:92–104.
40. Dong J, Viswanathan S, Adami E, Schafer S, Kuthubudeen FF, Widjaja AA, et al. Overturning the paradigm that IL6 signaling drives liver regrowth while shining light on a new therapeutic target for regenerative medicine. *bioRxiv* 2021. Available from: <https://www.biorxiv.org/content/10.1101/2021.04.05.438446v1>.
41. Bae GH, Lee SK, Kim HS, Lee M, Lee HY, Bae YS. Lysophosphatidic acid protects against acetaminophen-induced acute liver injury. *Exp Mol Med* 2017;**49**:e407.
42. Cressman DE, Greenbaum LE, DeAngelis RA, Ciliberto G, Furth EE, Poli V, et al. Liver failure and defective hepatocyte regeneration in interleukin-6-deficient mice. *Science* 1996;**274**:1379–83.
43. Selzner M, Camargo CA, Clavien PA. Ischemia impairs liver regeneration after major tissue loss in rodents: protective effects of interleukin-6. *Hepatology* 1999;**30**:469–75.
44. James LP, Lamps LW, McCullough S, Hinson JA. Interleukin 6 and hepatocyte regeneration in acetaminophen toxicity in the mouse. *Biochem Biophys Res Commun* 2003;**309**:857–63.
45. Río A, Gassull MA, Aldegue X, Ojanguren I, Cabré E, Fernández E. Reduced liver injury in the interleukin-6 knockout mice by chronic carbon tetrachloride administration. *Eur J Clin Invest* 2008;**38**:306–16.
46. Bajt ML, Knight TR, Farhood A, Jaeschke H. Scavenging peroxynitrite with glutathione promotes regeneration and enhances survival during acetaminophen-induced liver injury in mice. *J Pharmacol Exp Therapeut* 2003;**307**:67–73.
47. Shad BJ, Smeuninx B, Atherton PJ, Breen L. The mechanistic and ergogenic effects of phosphatidic acid in skeletal muscle. *Appl Physiol Nutr Metab* 2015;**40**:1233–41.